Electron Paramagnetic Resonance Investigations of a Kinetically Competent Intermediate Formed in Ribonucleotide Reduction: Evidence for a Thiyl Radical-Cob(II)alamin Interaction

G. J. Gerfen,*,†,‡ S. Licht,‡ J.-P. Willems,§ B. M. Hoffman,§ and J. Stubbe‡,#

Contribution from the Francis Bitter Magnet Laboratory, Department of Chemistry, and Department of Biology, Massachusetts Institute of Technology, Cambridge, Massachusetts 02139, and Department of Chemistry, Northwestern University, Evanston, Illinois 60208

Received February 5, 1996[⊗]

Abstract: The ribonucleoside triphosphate reductase (RTPR) from *Lactobacillus leichmannii* requires adenosylcobalamin (AdoCbl) as a cofactor to catalyze the conversion of nucleotides to deoxynucleotides. RTPR has previously been shown to catalyze the homolytic cleavage of the carbon−cobalt bond of AdoCbl, and the resulting paramagnetic species has been characterized by rapid freeze-quench EPR spectroscopy (Orme-Johnson, W. H.; Beinert, H.; Blakley, R. L. *J. Biol. Chem.* **1974**, *249*, 2338−2343. Licht, S.; Gerfen, G. J.; Stubbe, J. *Science* **1996**, *271*, 477−481). This study presents simulations of X- and Q-band EPR spectra of this intermediate. Modeling this species as a thiyl radical coupled to cob(II)alamin by electron-electron exchange and dipolar interactions yields reasonable fits to spectra obtained at both microwave frequencies, whereas simulations that employ a single-spin model do not. This modeling provides support for the intermediacy of a thiyl radical in this system. The techniques employed here may prove generally useful in simulation of similar spectra observed in other B_{12}-dependent enzyme systems.

Introduction

Ribonucleoside triphosphate reductase (RTPR) from *Lactobacillus leichmannii* catalyzes the adenosylcobalamin (AdoCbl)-dependent conversion of nucleoside triphosphates (NTPs) to deoxynucleoside triphosphates (dNTPs).[1,2] The protein is a monomer, $M_r = 82\,500$, that contains binding sites for the nucleotide substrates and deoxynucleotide allosteric effectors. Three cysteine residues (C408, C119, and C419) have been found to be essential for catalysis.[3] Two of these cysteines (C119 and C419) provide the reducing equivalents required for the reduction process (Figure 1), while a third cysteine (C408) is hypothesized to be oxidized to a thiyl radical that initiates nucleotide reduction by abstracting the 3′ hydrogen from the substrate.

In addition to nucleotide reduction, the enzyme also catalyzes an unusual exchange reaction in which tritium from [5′-^{3}H]-AdoCbl is transferred to the solvent.[4,5] This process, which can take place in the absence of substrate, requires an allosteric effector and the reduced form of RTPR and occurs with a rate constant 20% that of the rate constant for nucleotide reduction (Figure 1).[6]

Both the exchange reaction and nucleotide reduction have been studied extensively in the early 1970s by rapid kinetic techniques. Tamao and Blakley[7] used stopped-flow UV−visible spectroscopy to characterize an intermediate formed in a kinetically competent fashion in both the exchange and reduction reactions, while Orme-Johnson *et al.*[8] characterized the novel EPR spectrum of this intermediate using rapid freeze quench (RFQ) techniques. The EPR spectrum of this intermediate differs dramatically from that of cob(II)alamin bound to the enzyme in the presence of 5′-deoxyadenosine:[9] while cob(II)-alamin has $g_\perp = 2.23$, $g_\parallel = 2.0$, and a cobalt hyperfine splitting ($A_\parallel$) of 110 Gauss, the intermediate has an effective *g*-value of 2.12 and a cobalt hyperfine splitting of 50 Gauss.[8]

Orme-Johnson *et al.* suggested that this intermediate might be composed of 5′-deoxyadenosyl radical (5′-dA•) and cob(II)-alamin, the expected products of homolysis of the carbon−cobalt bond of AdoCbl. However, they also observed that the use of [5′-^{2}H]- and [5′-^{13}C]-AdoCbl failed to alter the EPR spectrum of the intermediate, as might have been expected if the hyperfine splittings arising from 5′-dA• were observable in the spectrum. Although several investigators speculated that the observed EPR spectrum could be accounted for by dipolar and exchange coupling between an organic radical and cob(II)alamin,[10−12] no spectral fits were reported.

In 1986 studies of Ashley *et al.*[13] laid the foundation for a new hypothesis for the identity of the intermediate. Investigating nucleotide reduction using [3′-^{3}H]-NTPs, they demonstrated

* Corresponding author.
† Francis Bitter Magnet Laboratory.
‡ Department of Chemistry, MIT.
# Department of Biology, MIT.
§ Department of Chemistry, Northwestern University.
⊗ Abstract published in *Advance ACS Abstracts,* August 1, 1996.

(1) Stubbe, J. *Adv. Enzymol. Relat. Areas Mol. Biol.* **1990**, *63*, 349−417.
(2) Reichard, P. *J. Biol. Chem.* **1993**, *268*, 8383−8386.
(3) Booker, S.; Licht, S.; Broderick, J.; Stubbe, J. *Biochemistry* **1994**, *33*, 12679−12685.
(4) Beck, W. S.; Abeles, R. H.; Robinson, W. G. *Biochem. Biophys. Research Commun.* **1966**, *25*, 421−425.
(5) Hogenkamp, H. P. C.; Ghambeer, R. K.; Brownson, C.; Blakley, R. L.; Vitols, E. *J. Biol. Chem.* **1968**, *243*, 799−808.
(6) Booker, S. Ph.D. Thesis, Massachusetts Institute of Technology, 1994.
(7) Tamao, Y.; Blakley, R. L. *Biochemistry* **1973**, *12*, 24−34.
(8) Orme-Johnson, W. H.; Beinert, H.; Blakley, R. L. *J. Biol. Chem.* **1974**, *249*, 2338−2343.
(9) Hamilton, J. A.; Yamada, R.; Blakley, R. L.; Hogenkamp, H. P. C.; Looney, F. D.; Winfield, M. E. *Biochemistry* **1971**, *10*, 347−355.
(10) Pilbrow, J. R. In *B12*; Dolphin, D., Ed.; Wiley-Interscience: New York, 1982; Vol. 1, pp 431−462.
(11) Blakley, R. L.; Orme-Johnson, W. H.; Bozdech, J. M. *Biochemistry* **1979**, *18*, 2335−2339.
(12) Ghanekar, V. D.; Lin, R. J.; Coffman, R. E.; Blakley, R. L. *Biochem. Biophys. Res. Commun.* **1981**, *101*, 215−221.
(13) Ashley, G. W.; Harris, G.; Stubbe, J. *J. Biol. Chem.* **1986**, *261*, 3958−3964.

S0002-7863(96)00363-0 CCC: $12.00

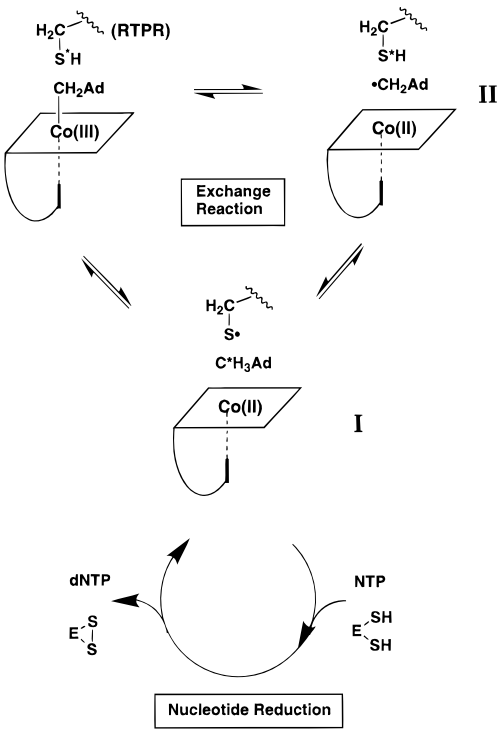

Figure 1. The intermediate trapped by rapid freeze quench techniques and its proposed role in ribonucleotide reduction. The asterisks mark the solvent-derived hydrogen of a cysteine thiol, which exchanges with the 5′ hydrogens of AdoCbl in the RTPR-catalyzed exchange reaction. Species I is the intermediate trapped by rapid freeze quench techniques. Species II is a putative intermediate containing a 5′-dA•, which has not, to date, been observed. $E(SH)_2$ indicates the two cysteines of RTPR oxidized concomitant with substrate reduction.

that 5′-dA• did not abstract a hydrogen atom directly from the substrate, thus requiring the proposal that the function of AdoCbl was to generate a protein radical on RTPR from a monoprotic amino acid residue within the active site of the enzyme. Based on extensive biochemical studies on both the *L. leichmannii* reductase and the ribonucleotide reductase isolated from *E. coli*, the monoprotic protein radical was proposed to be a thiyl radical.[1] Thus, the EPR spectrum of the intermediate observed by Orme-Johnson *et al.* could result from a thiyl radical exchange coupled to cob(II)alamin (Figure 1). To test this hypothesis, [β-^{2}H]-labeled cysteine was incorporated into RTPR, and the intermediate was again examined by RFQ-EPR spectroscopy.[14] The hyperfine features of the cobalt were narrower than those observed with unlabeled RTPR, providing the first direct support for a contribution of a thiyl radical to the observed signal.

With this new insight into the composition of the intermediate, efforts have now been renewed to simulate its spectrum. This report shows that the unusual spectral features of the intermediate observed at both 9 (Figure 2) and 35 GHz (Figure 4) EPR frequencies are accounted for by simulations that use *g*-values and hyperfine coupling constants appropriate for both a thiyl radical and cob(II)alamin within a model that includes exchange and dipolar couplings between the unpaired spins. This model affords better fits than alternative models, such as a single cob(II)alamin species or a coupled-spin system incorporating a carbon-centered radical. The successful simulation of spectra taken at different frequencies, together with the previously reported results of EPR studies incorporating [β-$^2H_2$]cysteine into the protein, provide strong support for proposal that the intermediate is composed of cob(II)alamin interacting with a thiyl radical.[14]

(14) Licht, S.; Gerfen, G. J.; Stubbe, J. *Science* **1996**, *271*, 477−481.

Experimental Section

Samples containing the paramagnetic intermediate were generated by rapidly mixing RTPR with AdoCbl in the presence of the allosteric effector dGTP, quenching the reaction in isopentane at −140 °C, and recording EPR spectra, as described previously.[14] Quenching into Q-band tubes was accomplished as described by Burdi *et al.*[15] The preparation of RTPR with [β-^{2}H]cysteine was previously described, and the incorporation was found to be 60%.[14] Continuous-wave EPR spectra were recorded at 2 K on a modified Varian E109 EPR spectrometer equipped with an E110 35 GHz microwave bridge in the dispersion mode. A 100 kHz field modulation was used under conditions of rapid passage as described elsewhere.[16] In this detection scheme the signal approximates the undifferentiated EPR absorption envelope. Pseudomodulation of the saturated dispersion spectra was carried out using the method of Hyde *et al.*[17] Goodness of fit of the simulations was determined by inspection.

Simulation Procedure

The EPR simulations incorporate two electron spin 1/2 species (S^α and S^β) interacting via isotropic exchange coupling (J_{ex}) and a dipolar coupling (**D**, with principal values defined as $-\mathbf{D}/3 + \mathbf{E}$, $-\mathbf{D}/3 - \mathbf{E}$, $+2\mathbf{D}$.[18] In addition, each electron spin is coupled to a nucleus of arbitrary spin (**I**) via an electron-nuclear hyperfine interaction (**A**). The total spin Hamilitonian H can be expressed as a sum of Hamiltonians for electronic (H_e), nuclear (H_n), and electron-nuclear (H_{en}) interactions

$$H = H_e + H_n + H_{en}$$

in which

$$H_e = |\mu_e|\mathbf{B}_0\cdot\mathbf{g}^\alpha\cdot\mathbf{S}^\alpha + |\mu_e|\mathbf{B}_0\cdot\mathbf{g}^\beta\cdot\mathbf{S}^\beta - J_{ex}\mathbf{S}^\alpha\cdot\mathbf{S}^\beta + 2\mathbf{S}^\alpha\cdot\mathbf{D}\cdot\mathbf{S}^\beta$$

$$H_n = -|\mu_n|g_n^\alpha\mathbf{B}_0\cdot\mathbf{I}^\alpha - |\mu_n|g_n^\beta\mathbf{B}_0\cdot\mathbf{I}^\beta$$

$$H_{en} = \mathbf{S}^\alpha\cdot\mathbf{A}^\alpha\cdot\mathbf{I}^\alpha + \mathbf{S}^\beta\cdot\mathbf{A}^\beta\cdot\mathbf{I}^\beta$$

$\mathbf{B}_0$ is the applied static magnetic field; μ_e and μ_n are the electron and nuclear magnetic moments, respectively. Because the H_e typically contains at least one interaction which is much greater in energy compared to H_n or H_{en}, this Hamiltonian can be treated in isolation and solved exactly by matrix diagonalization to obtain the energies and eigenvectors of each of the 4 electron-spin manifolds.[19] Transition probabilities between electron-spin manifolds are determined using these eigenvectors and the Hamiltonian (H_1)

$$H_1 \alpha \mathbf{B}_1\cdot\mathbf{g}^\alpha\cdot\mathbf{S}^\alpha + \mathbf{B}_1\cdot\mathbf{g}^\beta\cdot\mathbf{S}^\beta$$

in which the microwave field B_1 can be oriented parallel or perpendicular to B_0. The expectation values of the α and β electron spin for the jth manifold $\langle S\rangle_j^{(\alpha,\beta)}$ are used to calculate the effective field along which the nuclei are quantized:

(15) Burdi, D.; Sturgeon, B. E.; Tong, W. H.; Stubbe, J.; Hoffman, B. M. *J. Am. Chem. Soc.* **1996**, *118*, 281−282.

(16) Werst, M. M.; Davoust, C. E.; Hoffman, B. M. *J. Am. Chem. Soc.* **1991**, *113*, 1533−1538.

(17) Hyde, J. S.; Jesmanowiscz, A.; Ratke, J. J.; Antholine, W. E. *J. Magn. Reson.* **1992**, *96*, 1−13.

(18) Abragahm, A.; Bleaney, B. *Electron Paramagnetic Resonance of Transition Ions*; Dover: New York, 1970.

(19) In the simulations presented here, the Zeeman interactions (10^1 GHz) are much greater than the largest contribution to H_{en} and H_n (10^2 MHz) and therefore this form of the high field approximation is valid, independent of the size of the exchange coupling or zero field interaction.

$$B_{ef,j}^{(\alpha,\beta)} = \left| \frac{\langle \mathbf{S} \rangle_j^{(\alpha,\beta)} \cdot \mathbf{A}^{(\alpha,\beta)}}{\mu_n g_n^{(\alpha,\beta)}} + \mathbf{B}_0 \right|$$

The resulting nuclear sublevel energies (given by $\mu_n g_n^{(\alpha,\beta)} B_{ef,j}^{(\alpha,\beta)} m_I^{(\alpha,\beta)}$ in which $m_I^{(\alpha,\beta)}$ is the zth component of the magnetization of the α or β nuclear spin) are then combined with the electron spin manifold energies to obtain the total energy of each level. Transitions are included only for $\Delta m_I^{(\alpha,\beta)} = 0$. Calculations are performed in the magnetic field domain using a fixed EPR frequency.

Results

Our previous RFQ EPR experiments at 9 GHz carried out with RTPR and [β-^{2}H]cysteine-labeled RTPR revealed spectra of an intermediate involved in both the exchange and reduction reactions (reproduced in Figure 2A,C). Figure 2B,D respectively, present fits to this experimental data using the simulation protocol described above for two interacting electron spins (α and β), with parameters given in Table 1. Species α was modeled as enzyme-bound cob(II)alamin, and therefore the principal g-values and the cobalt nuclear hyperfine coupling matrix consistent with this species bound to RTPR were used (Table 1).[10]

Species β was taken as a thiyl radical and g-values for this species were selected accordingly. In addition, a single β-proton hyperfine coupling constant was selected for the simulations based on the single crystal EPR/ENDOR studies of cysteinyl radical in which the orientation of the methylene side chain was such that only a single proton splitting was observed.[20] The validity of this choice was assessed by varying the hyperfine coupling until the spectral narrowing observed upon simulation of the deuteriated sample matched the features of the experimentally observed spectrum. The best fit resulted from a value of about 3 mT, which is approximately the value measured in the single-crystal ENDOR study.

Simulations with a Thiyl Radical/Cob(II)alamin Model. To obtain the spectral fits shown in Figure 2B,D, an exchange coupling, $|J_{ex}|$, of >0.45 cm^{-1} as well as **D** values that are within the range of 1×10^{-2}–2×10^{-2} cm^{-1} (Table 1) were required. These simulations reproduce the general features of the experimentally acquired X-band EPR spectrum, which include the "effective" g-value of 2.12, the spectral width and intensities, and the scaling of the cobalt hyperfine splitting by approximately a factor of two (from ~110 G in cob(II)alamin to ~50 G in the intermediate for A_{33}) (compare Figure 2A,B). Furthermore, simulated replacement of the thiyl radical β−proton with a deuteron ($I = 1$, $g_{nD}/g_{nH} = 0.154$) produces the experimentally observed line-narrowing (compare Figure 2 parts C and D).

The effects of exchange coupling (J_{ex}) on the EPR spectra of a variety of systems have been previously described.[18,21−24] The influence of J_{ex} on our system of a thiyl radical interacting with cob(II)alamin is shown in Figure 3. Spectrum 3A is a simulation of the noninteracting ($|J_{ex}| = \mathbf{D} = 0$) thiyl radical and cob(II)alamin species using parameters listed in Table 1. The main features of the spectrum are the relatively intense

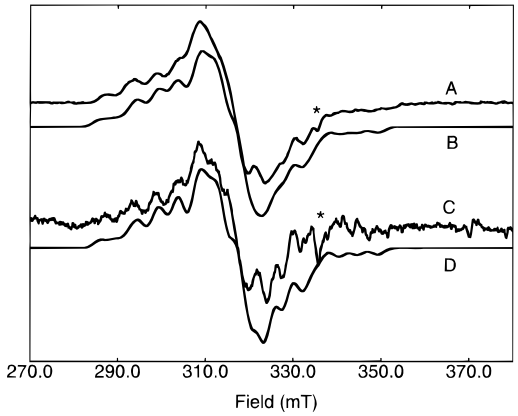

Figure 2. X-band EPR spectra and simulations of I in the presence of [β-^{1}H$_2$]cysteine-labeled RTPR (A and B) and [β-^{2}H$_2$]-cysteine-labeled RTPR (C and D). A and C: Experimental spectra obtained as previously reported.[14] Spectrometer frequency 9.41 GHz; temperature 100 K; microwave power 10 mW; modulation frequency 100 kHz; modulation amplitude 0.4 mT; time constant 1.3 s; scan time 671 s; each experimental spectrum is the sum of ten scans. The starred feature is a contaminant present in variable amounts in the freeze-quenched samples. B and D: Simulations using parameters in Table 1 and a Gaussian line broadening of 3.0 mT. B: 100% proton simulation; D: 60:40 sum of deuteron:proton simulations.

peaks in the "perpendicular" region for cob(II)alamin ($g_\perp^{Co} \approx 2.23$) and for the thiyl radical ($g_\perp^{S} \approx 2.0$). Upon introduction of the exchange coupling, these peaks separate into "inner" and "outer" transitions. The outer transitions are split from the corresponding inner transitions by $|J_{ex}|$ and lose intensity as $|J_{ex}|$ is increased, while the inner transitions move together and eventually merge at $|J_{ex}| \approx |(g_\perp^{Co} - g_\perp^{S})\beta_e B_0/hc|$. The resolved cobalt hyperfine splitting also scales inversely with $|J_{ex}|$ until it reaches the limiting value of $A^{Co}/2$ for $|J_{ex}| > |(g_\perp^{Co} - g_\perp^{S})\beta_e B_0/hc|$. In order to reproduce the observed line shape and cobalt hyperfine splittings as well as to decrease the intensities of the outer transitions that are not observed experimentally, $|J_{ex}| > 0.45$ cm^{-1} (Figure 3D) is required. The spectroscopic position (effective g-value) and the size of the cobalt hyperfine splitting observed for the kinetically competent intermediate, as illustrated in Figure 3, thus require the presence of an exchange coupling between the paramagnetic species.

A stringent test of a model which includes electron−electron interactions involves the successful fitting of spectra obtained at several EPR frequencies. The effects of field-dependent (Zeeman interaction) and -independent (exchange coupling, electron−electron dipole interaction, hyperfine coupling) terms in the Hamiltonian must be reproduced with a consistent parameter set at all magnetic field strengths.[25] The spectrum of the intermediate was therefore acquired at 35 GHz (Figure 4A) and simulated (Figure 4B) using the same parameter set (Table 1) that was used to simulate the 9 GHz spectrum (Figure 2). The Q-band simulation accurately reproduces the overall spectroscopic position, width, and line shape of the experimentally obtained spectrum, supporting the hypothesis for the structure of the intermediate.

An additional means to characterize an electron−electron dipole coupled system is via the observation of a half field or "$\Delta M = 2$" EPR transition.[18,21,26,27] Attempts to observe this transition for our intermediate in the perpendicular B_1 mode have, however, thus far been unsuccessful. Simulations indicate that the maximum intensity of this transition is expected to be

(20) Kou, W. W. H.; Box, H. C. *J. Chem. Phys.* **1976**, *64*, 3060−3062.
(21) Eaton, G. R.; Eaton, S. S. In *Biological Magnetic Resonance*; Berliner, L. J. Reuben, J., Ed.; Plenum Press: New York, 1989; Vol. 8, pp 339-397.
(22) Smith, T. D.; Pilbrow, J. R. *Coord. Chem. Rev.* **1974**, *13*, 173−278.
(23) Schepler, K. L.; Dunham, W. R.; Sands, R. H.; Fee, J. A.; Abeles, R. H. *Biochim. Biophys. Acta* **1975**, *397*, 510−518.
(24) Buettner, G. R.; Coffman, R. E. *Biochim. Biophys. Acta* **1977**, *480*, 495−505.
(25) Eaton, S. S.; More, K. M.; DuBois, D. L.; Boymel, P. M.; Eaton, G. R. *J. Magn. Reson.* **1980**, *41*, 150−157.

Table 1. Parameters Used for X- and Q-Band Simulations of Intermediate I[a]

	g_1	g_2	g_3	A_x	A_y	A_z	ϕ_{hyp}[b]	θ_{hyp}[b]	ψ_{hyp}[b]
cob(II) alamin	2.230	2.235	2.009	15.0[c]	36.0[c]	310.0[c]	50	0	0
thiyl radical	1.984	2.001	2.230	107.0[d]	98.8[d]	96.4[d]	−141[e]	17[e]	20[e]
	J_{ex}	**D**	E	$\phi_{D_{ip}}$[g]	$\theta_{D_{ip}}$[f]	$\psi_{D_{ip}}$[f]	ϕ_g[g]	θ_g[g]	ψ_g[g]
	−41700	117	33	60	25	0	25	0	0

[a] A in MHz; J_{ex}, **D**, and E in 10^{-4} cm^{-1}. Euler angles, in deg, are defined as in Goldstein (Herbert Goldstein, Classical Mechanics, Addison Wesley, Reading MA, 1967). [b] Relates each hyperfine interaction principal axis system to the respective g-principal axis system. [c] Hyperfine coupling constants (MHz) for cobalt nucleus. [d] Hyperfine coupling constant (MHz) for β-methylene proton. Simulations of deuterated species used this value multiplied by 0.1535. [e] The approximately isotropic nature of the hyperfine interaction of the β-methylene proton renders the simulation insensitive to these angles. Values used were arbitrarily set to those reported for cysteinyl radical.[20] [f] Relates dipole coupling prinicpal axes to cobalt g-principal axes. [g] Relates thiyl radical g principal axis system to cobalt g principal axis system.

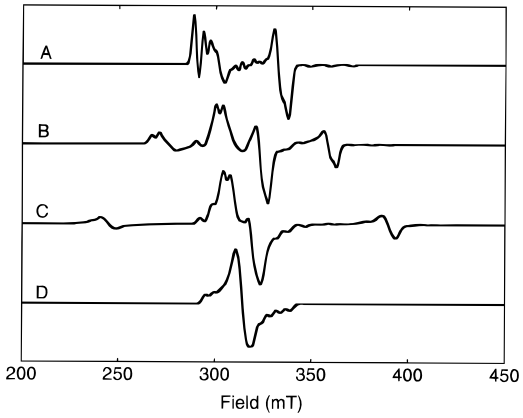

Figure 3. X-band simulations of two electron spin 1/2 species illustrating the effects of the exchange coupling (J_{ex}). The parameters given in Table 1 are used in all simulations with the exception of D and E (set equal to 0), and J_{ex} is varied as follows: A, 0.0 cm^{-1}; B, −0.033 cm^1; C, −0.067 cm^{-1}; D, −4.17 cm^{-1}.

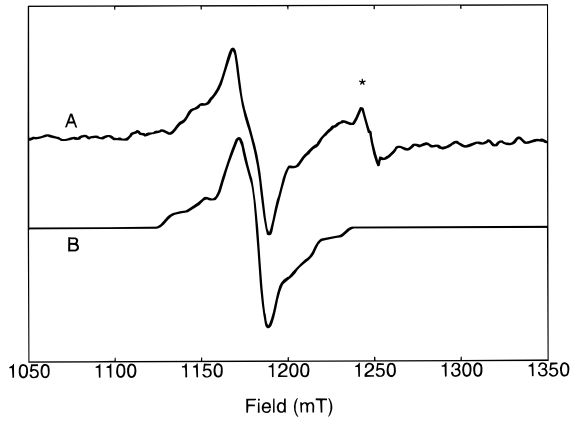

Figure 4. Q-band EPR spectrum and simulation of I. A: Experimental data of enzyme with [β-^{1}H$_2$]cysteine-labeled RTPR. The experimental conditions are identical to those previously described[14] and samples were prepared using the recently described method for obtaining RFQ ENDOR spectra.[15] Spectrometer frequency 34.93 GHz; temperature 2 K; modulation frequency 100 kHz; modulation amplitude 2 G; time constant 64 ms; scan time 240 s; the displayed spectrum is a pseudomodulation[17,46] of the sum of 16 saturated dispersion spectra. The starred feature is a contaminant present in variable amounts in the freeze-quenched samples. B: Simulation using parameters in Table 1. The calculated spectrum was convolved with a saturated dispersion line shape function[47] and pseudomodulated in a manner analogous to the experimental spectrum. The overall width of the convolved line shape function was approximately 5.2 mT.

two orders of magnitude less than that of the main transition. Since the buildup of intensity in this transition arises from its reduced dependence on the zero-field interaction anisotropy (relative to the main transition) and is partially offset by the substantial cobalt hyperfine interactions, our inability to detect this transition is not surprising. A further difficulty arises from the technical complications associated with the rapid freeze quenching method. The method requires spraying samples into cold liquid isopentane, which contains O_2. The O_2 contributes an EPR signal in the half-field region that can potentially obscure the detection of the desired signal.

Alternative Models. Two alternative structures have previously been considered as possibilities for the intermediate. Simulations were performed to test these options. First, the simulation protocol was used to investigate the hypothesis that the intermediate might include a 5′-dA• (Figure 1, intermediate II), although previous isotopic labeling studies indicated that this was probably not the case.[8,14] Use of nearly isotropic g-values typical of a 5′-dA•[8] or amino acid radicals (g-values in the range from 2.000 to 2.010) rather than the anisotropic **g**-matrix of the thiyl radical (Table 1) failed to achieve reasonable fits to the experimental data, lending further support for a thiyl radical as the major component of this intermediate.

The second option, suggested to us and previously proposed by others,[28] is that the spectrum of this intermediate could be modeled as a single electron spin 1/2 species (or a mixture of such species) rather than the exchange-coupled radical pair discussed above. For example, the proposal has been made that cob(II)alamin is in a strongly distorted octahedral environment with a cysteine thiolate ligated off-axis.[28] While this proposal is at odds with a large number of biochemical studies,[8,14] its viability was further investigated by simulation of its experimental spectra.

The simulation of the 9 GHz spectrum assuming this single electron spin 1/2 model (compare Figure 5A,B) was calculated using parameters from a similar figure previously presented by Pilbrow.[10] Although the fit appears reasonable, the g-values, hyperfine coupling constants, and principal axes orientations required to simulate the spectrum are unprecedented for cob(II)alamin and cob(II)inamide coordination complexes.[9,10,29−31] Moreover, the simulation fails to reproduce the intensities at the spectral edges. A simulation of the Q-band spectrum (compare Figure 5 (parts C and D)) using these same parameters completely fails to reproduce the overall spectral width and line shape. We thus conclude**,** as Pilbrow did based on X-band data,[10] that a single electron spin model is inadequate to describe the observed experimental data.

Discussion

Simulations of EPR spectra of the intermediate generated during the RTPR-catalyzed exchange and reduction reactions

(26) Coffman, R. E.; Ishikawa, Y.; Blakley, R. L.; Beinert, H.; Orme-Johnson, W. H. *Biochim. Biophys. Acta* **1976**, *444*, 307−319.
(27) Bayston, J. H.; Looney, F. D.; Pilbrow, J. R.; Winfield, M. E. *Biochemistry* **1970**, *9*, 2164−2172.
(28) Schrauzer, G. N.; Lee, L. P. *J. Am. Chem. Soc.* **1970**, *92*, 1551−1557.
(29) Jörin, E.; Schweiger, A.; Günthard, H. H. *Chem. Phys. Lett.* **1979**, *61*, 228−232.

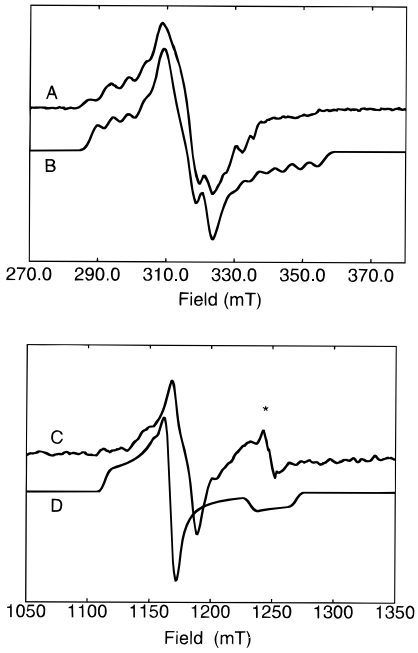

Figure 5. EPR spectra of the intermediate and simulations for a single electron spin 1/2 species. A and C: Identical to the spectra in Figure 2A and Figure 4A. B and D: Simulations assuming a single electron spin 1/2 species. Spectrum B is the simulated absorption spectrum with a Gaussian linebroadening function of 4.0 mT, while spectrum D is a pseudomodulated saturated dispersion signal with a linebroadening function of approximately 6.5 mT. The *g*-values (1.995, 2.198, 2.140) and cobalt hyperfine splitting constants (47.1 G, 53.5 G, 7.5 G) were taken from a similar figure published previously by Pilbrow.[10]

(Figure 1) support the assignment of this species as a protein-based thiyl radical interacting with cob(II)alamin. The simulations reproduce the unusual features of this spectrum, including its "effective *g*-value", the cobalt hyperfine splitting, and the effects of incorporation of β-deuterated cysteine into RTPR. Models in which the intermediate was postulated to result from 5′-dA• and cob(II)alamin or from a single cobalt(II) species were also investigated. Simulations of these models, however, were inadequate to account for the EPR spectra, in accord with earlier biochemical and spectroscopic results.[8,14]

The limiting values which can be set for both **D** and J_{ex} provide structural information regarding the cob(II)alamin-thiyl radical pair. As indicated in Table 1, reasonable fits to the data require **D** values that lie in the range of $1 \times 10^{-2}-2 \times 10^{-2}$ cm^{-1}. If the interaction giving rise to **D** is exclusively assigned to a dipolar coupling between point dipoles, this range provides a distance of approximately 5−7 Å between paramagnetic centers. However, since this interaction may also contain contributions from "pseudo-dipolar" terms arising from anisotropic exchange and spin orbit coupling,[22,32] and since electron delocalization may render the point dipole assumption inaccurate,[33] this distance determination must be considered an estimate.

The requirement for $|J_{ex}| > 0.45$ cm^{-1} to adequately reproduce the data at both X-band and Q-band (a value of -4.17 cm^{-1} was used in the simulations shown in Figures 2 and 4) indicates an interaction of the molecular orbitals containing the unpaired spins. The calculated range for J_{ex} is in agreement with the estimate of $|J_{ex}| \sim 1$ cm^{-1} obtained from the temperature dependence of the EPR signal intensity.[14]

Since exchange coupling between unpaired electrons may arise from direct orbital overlap or be mediated via the orbitals of intervening atoms, the magnitude of J_{ex} tends to decrease with increasing distance between the species.[21,22,34,35] The complexity of the interaction prevents the unique inference of structure from values of J_{ex}. However, in well characterized systems with $|J_{ex}| \geq 0.45$ cm^{-1}, distances between unpaired electrons are generally less than 8 Å unless the intervening bonding network is highly conjugated.[21,22,36,37] Based on these previous studies, an upper limit of 8 Å for the cob(II)alamin-thiyl radical can be assigned. This value is consistent with the distance estimates based on the value of the dipolar coupling parameter **D** and provides further evidence for the proximity of the two radical species in the enzyme.

The simulations (Figures 2 and 4) require a large number of adjustable parameters (Table 1), and there may be discrepancies between the assumed and actual *g* and *A* values for both cob(II)alamin and thiyl radical. Thus it is clear that a unique fit to the experimental data is not possible at this stage. However, as outlined below, these simulations have provided the framework for experiments that will lead to refinement of these parameters.

Fitting EPR spectra obtained at other EPR frequencies[25] (4, 95, 140, and 250 GHz) is another method for the refinement of Hamiltonian parameters and the structural information these parameters provide. Spectra recorded at lower frequencies should accentuate the effects of the zero field splitting and hyperfine interactions, while spectra obtained at higher frequencies will be more sensitive to *g*-values and will provide more precise limits on the value of J_{ex}. Further investigations of half-field transitions in the parallel B_1 mode[18,26,38] may also allow refinement of the zero field splitting interaction parameters. These experiments are in progress. Nonetheless, the success of the simulations shown in Figures 2 and 4 provides compelling evidence that the kinetically competent intermediate species in the RTPR catalyzed exchange and reduction reactions consists of a thiyl radical interacting with cob(II)alamin.

Finally, the simulation procedure described in this paper may be useful in the interpretation of EPR spectra of other radical pairs formed in biological systems. EPR spectra similar to those shown in Figure 2 for *L. leichmannii* ribonucleotide reductase have also recently been observed for other AdoCbl-dependent enzymes, such as glutamate mutase,[39,40] methyleneglutarate mutase,[40,41] and methylmalonyl-CoA mutase.[40,42−44] The results presented in this work support the claims that these spectra may

(30) Bleaney, B.; Bowers, K. D. *Proc. Roy. Soc. London Ser. A* **1952**, *21*, 451−465.
(31) Belford, R. L.; Chasteen, N. D.; So, H.; Tapscott, R. E. *J. Am. Chem. Soc.* **1969**, *91*, 4675−4680.
(32) Rajca, A. *Chem. Rev.* **1994**, *94*, 871−893.
(33) Forbes, M. D. E.; Bhagnt, K. *J. Am. Chem. Soc.* **1993**, *115*, 3382−3383.
(34) Eaton, G. R.; Eaton, S. S. *Acc. Chem. Res.* **1988**, *21*, 107−113.
(35) Matsumoto, T.; Ishido, T.; Koga, N.; Iwamura, H. *J. Am. Chem. Soc.* **1992**, *114*, 9952−9959.
(36) Wertz, J. E.; Bolton, J. R. *Electron Spin Resonance*; 2nd ed.; Chapman and Hall: New York, 1986.
(37) Bleaney, B. *Phil. Mag.* **1951**, *42*, 441.
(38) Eaton, S. S.; More, K. M.; Sawant, B. M.; Eaton, G. R. *J. Am. Chem. Soc.* **1983**, *105*, 6560−6567.
(39) Zelder, O.; Beatrix, B.; Leutbecher, U.; Buckel, W. *Eur. J. Biochem.* **1994**, *226*, 577−585.
(40) Beatrix, B.; Zelder, O.; Kroll, F. K.; Örlygsson, G.; Golding, B. T.; Buckel, W. *Angew. Chem., Int. Ed. Engl.* **1995**, *34*, 2398−2401.
(41) Michel, C.; Albracht, S. P. J.; Buckel, W. *Eur. J. Biochem.* **1992**, *205*, 767−773.
(42) Keep, N. H.; Smith, G. A.; Evans, M. C. W.; Diakun, G. P.; Leadlay, P. F. *Biochem. J.* **1993**, *295*, 387−392.
(43) Zhao, Y.; Abend, A.; Kunz, M.; Such, P.; Rétey, J. *Eur. J. Biochem.* **1994**, *225*, 891−896.
(44) Padmakumar, R.; Banerjee, R. *J. Biol. Chem.* **1995**, *270*, 9295−9300.

also arise from coupled cob(II)alamin-carbon center radical systems.[39−44] Simulations of these individual spectra are in progress.[45]

(45) Bothe, H.; Buckel, W.; Gerfen, G. J. Unpublished results.

(46) van der Donk, W. A.; Stubbe, J.; Gerfen, G. J.; Bellew, B. F.; Griffin, R. G. *J. Am. Chem. Soc.* **1995**, *117*, 8908−8916.

(47) Ammerlaan, C. A. J.; van der Wiel, A. *J. Magn. Reson.* **1976**, *21*, 387−396.

Acknowledgment. This work was supported by National Institutes of Health grants to J.S. (GM-29595), B.M.H. (HL-13531), and Robert G. Griffin (GM-38352 and RR-00995). G.J.G. acknowledges a postdoctoral fellowship from the American Cancer Society (PF-3668). S.L. is a Howard Hughes Medical Institute Predoctoral Fellow.

JA960363S